MEMOIRS

OF THE

COLLEGE OF SCIENCE

UNIVERSITY OF KYOTO

SERIES A

THE
PHYSICAL
SOCIETY

VOL. XXV. NO. 2.

OCTOBER 1949

KYOTO

Memoirs of the College of Science, University of Kyoto, Series A,
Vol. XXV, No. 2, Article 8, 1949.

On a Property of the Conjugate Net in Connexion with Generalized Projective Deformation

By

Joyo Kanitani

(Received August 6, 1947)

Consider a non-ruled surface S in a three-dimensional projective space. Associate to a generic point E of S a moving frame of reference $[E, E_1, E_2, E_3]$, of which the vertices E_1, E_2 lie on the tangent plane of S at E and the vertex E_3 is outside of this tangent plane. The movement of this frame is defined by the system of the equations of the form:

$$dE = dw_0^0 E + dw_0^i E_i,$$
$$dE_i = dw_i^0 E + dw_i^l E_l + dw_i^3 E_3, \quad (i = 1, 2)$$
$$dE_3 = dw_3^0 E + dw_3^l E_l + dw_3^3 E_3.$$

Choosing the vertices E_1, E_2 properly, we can make

$$dw_0^0 = 0, \quad dw_0^1 = dx^1, \quad dw_0^2 = dx^2,$$

where x^1, x^2 are the parameters on which the generic point E depends. Take the point E_3 so that the frame $[E, E_1, E_2, E_3]$ becomes a frame of Darboux, namely, the surface S referred to the frame $[E, E_1, E_2, E_3]$ is defined by the equation:

$$z^3 = \frac{1}{2} H_{ij} z^i z^j - \frac{1}{3} K_{ijl} z^i z^j z^l + \cdots\cdots\cdots\cdots,$$

where

$$H_{ij} z^i z^j = 0$$

gives the asymptotic tangents, while

$$K_{ijl} z^i z^j z^l = 0$$

gives the tangents of Darboux so that

$$H^{ij}K_{ijl} = 0.$$

Then, by choosing properly the common factor of the coordinates of the point E_3, we can make

$$dw_i^3 = H_{ij}dx^j, \quad dw_3^3 = 0,$$
$$dw_i^l = (K_{ij}^{\ l} + \Gamma_{ij}^{\ l})\, dw^j,$$

where Γ_{ijl} ($i, j, l = 1, 2$) are Christoffel's symbols with respect to the quadric from $H_{ij}dx^idx^j$.

We now regard the surface S as the space $\boldsymbol{R}_2$ with the connexion dw_α^β ($\alpha, \beta = 0, 1, 2$). If we develop any curve drawn from a point A on S into the tangent plane at A, defining the moving frame [A, A_1, A_2] by means of the equations

$$dA_\alpha = dw_\alpha^\beta A_\beta \quad (A_0 \equiv A\,;\, \alpha = 0, 1, 2),$$

and giving to A, A_1, A_2 the same initial values as those of E, E_1, E_2, then the infinitely small variations of E, E_1, E_2 are obtained by projecting the homologous variations of A, A_1, A_2 from the point E_3.

If we take as the point E_3 another point satisfying the above-mentioned condition, namely, a point on the line EE_3, *the space corresponding to the new center of projection is projectively deformable*[1] *to the original space.*

Now suppose that the parameter curves upon S form a conjugate net. Then, by choosing the common factor of the coordinates of the point E, we can make

$$K_{11}^{\ 2} + \Gamma_{11}^{\ 2} = 0,$$

so that the point E_3 becomes a point on the plane osculating at E to the curve $x^2 = \text{const}$ passing through this point.

Thus, we get

$$dE = dx^iE_i,$$
$$dE_1 = dw_1^0E + dw_1^1E_1 + (K_{12}^{\ 2} + \Gamma_{12}^{\ 2})\, dx^2E_2.$$

The Laplace transform on the line $E\,E_1$ is expressed by

$$E_1 - (K_{12}^{\ 2} + \Gamma_{12}^{\ 2})\, E.$$

---

1. J. Kanitani: On a generalisation of the projective deformation, This Memoirs, Vol. **25**, p. 23.

We have, therefore, the following proposition.

Let S be a non-ruled surface in a three-dimensional projective space, and A be a generic point of this surface. Consider a family of non-asymptotic curves upon S. Denote by l the tangent at A to the curve L passing through A and belonging to this family. Associate to S a projective connexion obtained by the projection from a point on the osculating plane of L at A. Then, the curves under consideration become geodesic lines for the space $\boldsymbol{R}_2$ with the connexion thus determined and consequently, this space can be so plunged[2] into a four-dimensional projective space that it becomes a ruled surface whose generating lines correspond to these geodesic lines and that, at a particular position of A, the characteristic of the envelope of the tangent hyperplane along generating line intersects the axis of projection. *The stationary point corresponding to this position of A, coincides with the Laplace transform of A on l with respect to the conjugate net of which the family under consideration forms a part.*

2. J. Kanitani: *loc. cit.*

Memoirs of the College of Science, University of Kyoto, Series A,
Vol. XXV, No. 2, Article 9, 1949.

On the Structure of Inter-crystalline Boundaries of Metals. II

By

Masaharu Kabata

(Received August 10, 1945)

---

§ V. *The Groove formed at the Inter-crystalline Boundary.* As stated already, when a metal is heated to a temperature lower by less than $10^0 \sim 20^0$C below its melting point, the liquid layer is formed at the inter-crystalline boundary, and it manifests as a groove when the test piece is cooled to the room temperature. However, the cooling is not necessary to form the groove. When the surface of the test piece in the furnace is looked with a magnifying glass through a glass window set on the wall of the furnace, we can detect that the groove is formed suddenly when the temperature reached to the lowest temperature above which the fluidification of the inter-crystalline boundary has been found to take place. Thus, the formation of the inter-crystalline groove does not require any long continued heating, but only a few seconds heating at the required temperature is sufficient to form it. A prolonged heating and a gradual cooling have only the effect to broaden the groove, and for the formation itself of the groove the heating even for a very short time at the required temperature, as was stated before, is sufficient.

Prof. U. Yoshida and Mr. K. Koyanagi supposed that the inter-crystalline groove is formed by the enhanced evaporation of the inter-crystalline liquid layer. But, the present observation that the inter-crystalline groove is formed by the heating at the required temperature only for a very short time denies their supposition. Further, when a metal is heated in the air, as in the present experiments, it must be considered to be covered by a comparatively thick oxide film which hinders a rapid evaporation of the inter-crystalline liquid layer. This fact is also unfavourable for the evaporation theory. Actually, the formation of the inter-crystalline groove does not depend upon

whether the metal is heated in the air or in vacuum.

Another reason for the formation of the inter-crystalline groove, which is next to be considered, is the expansion (contraction with Bi) caused by the thickening of the inter-crystalline liquid layer by heating and the contraction (expansion with Bi) due to the crystallization of the liquid layer by cooling. With regard to this point various experiments were made. First, among the single crystal test piece of Sn, Pb and Al in the form of rectangular plate, such specimens were selected that the boundary between two neighbouring crystals runs in transversal direction of the test piece. These specimens were heated to the required temperature and then cooled in the furnace, by laying horizontally on a flat stand or rollers so that they can expand or contract freely, or by hanging vertically in the furnace. But, no difference in the breadth and the depth of the grooves could be detected in these three cases. Next, with the specimens of the same kind as above, the distances between two points marked, once very closely and then remotely, on both sides of the inter-crystalline boundary were measured very accurately with a microscope before and after the heating to form the inter-crystalline boundary, and examined whether some expansion or contraction of the test piece had arisen in the direction perpendicular to the inter-crystalline boundary. If the groove be formed by the cause as is considering now, the excess mass forced out by the formation of the groove of considerable size should be spent in expanding the test piece in a detectable degree. But, the measurement did not show any trace of such expansion or contraction, and does not agree with the expansion and contraction theory. Further, the writer carried out a similar measurement with test pieces consisted of comparatively large number of small crystals, but any trace of the expansion or compression by the formation of the groove at the inter-crystalline boundaries could not be detected. If the expansion and contraction theory would be correct, we are to expect that the outer boundary of a crystal which is entirely surrounded by neighbouring crystal, would be grooved. But, the fact contradicts this expectation, and the grooves are always formed at inter-crystalline boundaries of all kinds. Of course, the writer admits, as will be stated later, the presence of some effects of the expansion and contraction on the formation and the shape of the inter-crystalline boundary; but he believes that the expansion and contraction which happens by the formation of the groove is not an essential cause for its formation. When, by the heating up of a test

piece in a furnace, its surface is looked with a magnifying glass through a glass window set on the wall of the furnace, we can detect that at the same time as the inter-crystalline groove is formed suddenly at a certain temperature, the part of the outer surface of the test piece in the neighbourhood of groove pulsates. As already mentioned, the fluidification of the outer surface and of the inter-crystalline boundary begins at the same lowest temperature. Considering from this and the pulsation of the outer surface of the test piece as stated above, it may be legitimately imagined that the inter-crystalline groove is formed by the drawing out of the inter-crystalline liquid layer into the outer surface (probably beneath the oxide film) of the test piece by the action of the surface tension. When the surface of a test piece on which the inter-crystalline grooves are formed is inspected closely, we can detect that the sharp vertices and edges of the crystals is rounded and the surface looks like to be covered by a rather solidified layer of the melt. Fig. 1, Plate II is the photograph of an aluminium test piece which was heated to a comparatively high temperature and has wide grooves on its surface, and we can see clearly wavy wrinkles on its surface. This seems to suggest that the inter-crystalline liquid layer is sucked beneath the oxide film covering the outer surface of the test piece and is in accord with the bulging of the lower end of the test piece, as stated before, when it is suspended and heated sufficiently in a furnace.

The writer made his experiments on the formation of inter-crystalline grooves with bismuth too. Differing from other metals, bismuth expands by crystallization, and an effect which is different from the case of other metals is expected to be present in the formation of the inter-crystalline grooves.

(a) The case of sudden cooling : A test piece of bismuth (BI), which was defined in § II, was suspended and heated at 265°C for 5 minutes in a vertical furnace, and then it was cooled suddenly by dropping it into the water under the furnace. The appearance of the inter-crystalline boundary of the specimen thus cooled is shown in Fig. 2, Plate II. The inter-crystalline boundary in this case protruded instead of becoming a groove, and at the summit of such protuberance some small spheres were formed due probably to the eruption of the inter-crystalline liquid layer.

(b) The case of slow cooling : A test piece of bismuth (BI) is heated in the same way as above. After having been kept at 265°C

for 5 minutes, the test piece was cooled slowly in the furnace by cutting the electric current through the furnace. As is shown in Fig. 3, Plate II, the inter-crystalline boundary became grooved in this case as in the case of other metals; and a few small spheres, much less in number than in the former case, were formed in the groove. In the case of slow cooling, both exterior and interior parts cool rather uniformly, and the expansion due to the crystallization of the inter-crystalline liquid layer will be distributed rather evenly over the whole parts of the test piece and will not much strain locally the inter-crystalline boundary.

Consequently the inter-crystalline groove formed at high temperature is supposed to be retained after cooling. Differently from this, the exterior part of the test piece crystallizes firstly in the case of rapid cooling, by leaving the interior of the inter-crystalline liquid layer unsolidified, and the expansion due to the crystallization of the exterior part, gives rise to the protrusion of that part as is shown in Fig. 2, Plate II. When such a crystallization of the exterior part proceeds inwards, the expansion accompanying it gives forth the eruption, as small spheres, of the melt remaining still unsolidified in the interior through some weak localities in the solidified exterior part. In the case of slow cooling, the inward advance of the solidification also happens, though more slowly and the eruptions of the unsolidified part of the interior as small spheres is also expected to take place in much smaller number. Considering in such a way, the formation of such small metal spheres by eruption can be regarded as another strong evidence, in addition to the result of X-ray examination for the existence of the inter-crystalline liquid layer at the temperatures lower than the melting point of the metal.

Next with tin and bismuth, the depth and the shape of the inter-crystalline groove were investigated by means of an Ultropak microscope and the cross-sectional view thus obtained is shown in Figs. 7 and 8.

The test piece of tin, investigated in the case of Fig. 7, was in the form of plate. After having been heated at 223°C for 3 minutes in horizontal position in a furnace, it was cooled slowly in the furnace.

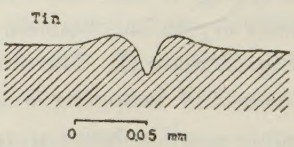

Fig. 7

In the case of bismuth shown in Fig. 8, the surface of a rod obtained by casting was etched so slightly that the inter-crystalline boundary was clearly visible without forming any

groove. Then the rod was sealed in an evacuated glass tube, heated at 265°C for 5 hr in horizontal position in a furnace, and cooled very slowly by lowering the temperature of the furnace gradually. As is evident from the figures the both sides of the groove are swollen up in both case, only slightly in the case of tin and especially remarkably on one side in the case of bismuth. This peculiarity of bismuth is not limited to this case shown in Fig. 8, but was observed almost in all cases examined by the writer. According to the writer's view such swelling up of both sides of the groove in both cases is due partly to the sucking up of the melt at the inter-crystalline boundary to the outer surface of the test piece in the immediate neighbourhood of the groove. There is another factor in the case of bismuth that the expansion due to the crystallization of the inter-crystalline liquid layer by the cooling after heating affects a considerable pressure upon the neighbouring portion. This pressure forces out, on one hand, the still remaining melt in the interior as small spheres as stated before, and on the other hand, it deforms plastically the neighbouring crystals and causes them to bluge outwards. As stated before, the bluges formed on both sides of the groove is generally uneven. The crystal axes and accordingly the slip planes and the slip direction of two crystals on both sides of the groove are generally in different directions, and consequently the easiness to suffer plastic deformation due to the crystallization of the inter-crystalline liquid layer is different, so that uneven bluges are formed on both sides of the groove.

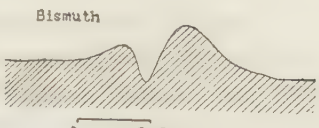

Fig. 8

§ VI *Displacement of the Inter-crystalline Boundary by Recrystallization.* As mentioned before, Prof. U. Yoshida and Mr. K. Koyanagi considered the recrystallization phenomenon of metals as to take place by the growth of the crystal nuclei formed in the inter-crystalline liquid layer by consuming the old strained crystallites by means of an intermediary action of the inter-crystalline liquid layer. If their consideration is correct, then when the recrystallization is made to occur rapidly at such high temperature as to bring forth the inter-crystalline groove, an interesting question arises whether the displacement of the inter-crystalline groove can be detected. The writer's experiments on this point are very insufficient at present. But a trace of such displacement of the inter-crystalline groove at high temperature could be detected.

Since, when a worked test piece of a metal is recrystallized at once by heating it suddenly to high temperature, the displacement of the inter-crystalline boundaries will be too much complicated, the writer performed the recrystallization in two steps: Firstly, the recrystallization was carried out at a comparatively low temperature so that the boundaries between new large crystals obtained by recrystallization are not grooved and that the recrystallization is almost but not perfectly completed. Next, the test piece, after having been recrystallized firstly, was heated suddenly for a short time at such high temperature as the inter-crystalline grooves are to be obtained; and by comparing the photographs taken before and after this heating the displacement of the inter-crystalline grooves was inspected.

The recrystallization at high temperature proceeds very rapidly, and consequently the displacement of the inter-crystalline grooves too. In the present experiment, the furnace provided with a narrow slit at its upper end, as is shown in Fig. 9, was used. The slit was kept open always and was so narrow that only the test piece can pass freely through it longitudinally, and that the temperature in the furnace does not fluctuate in any detectable degree by putting in and taking out the test piece. By keeping the temperature in the furnace at a desired high degree, the test piece was put into the furnace, and heated for a few minutes, and then it was taken out and cooled in the air.

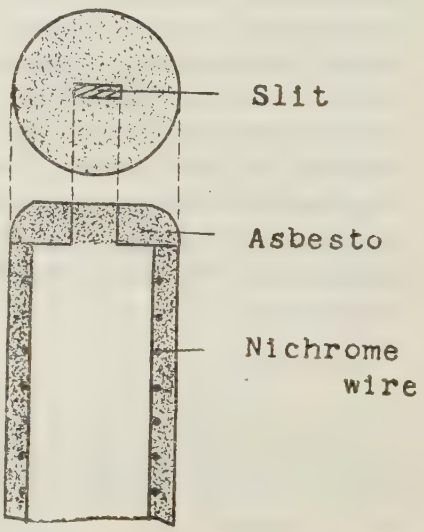

Fig. 9

The experiments were made with tin and aluminium. In the case of tin, an uncrystallized test piece having the same size as (SR), which has been defined in the previous report, was etched with concentrated hydrochloric acid, subjected to a rolling of 10%, and was then recrystallized for the first time by heating for 5 minutes at 210°C. With such heating the recrystallization was almost but not entirely completed.

After taking the photograph of the inter-crystalline boundaries of the test piece thus recrystallized firstly, the temperature of furnace

was raised to and kept at 224°C; and the test piece was heated for 3 minutes at this temperature and was then cooled in the air. The inter-crystalline grooves, formed on the surface of the test piece recrystallized thus for the second time, are shown in Figs. 5 (a) and 5 (b) in Plate II. In Fig. 5 (a), the groove running down vertically is formed by the second heating at the crystal boundary developed by the first heating, and the neighbouring part appearing white in a shape of wide band in the photograph is the trace traversed by the inter-crystalline boundary by the second heating and in the dark portion at the left end of the white band there situates the new inter-crystalline groove formed by the second heating at the final position of the displaced inter-crystalline boundary, though it is invisible in the photograph by unsuitable illumination. Fig. 5 (b) is the photograph taken to make this invisible groove visible by different illumination, and the one running down from the intersection of three grooves meeting at the upper part of the photograph, is this groove. Moreover, the other two grooves meeting at the upper part become clearer in this figure in place of the disapearance of the first groove which had appeared clearly in Fig. 5 (a). If the displacement of the inter-crystalline boundary takes place after its becoming a groove, then the part of the surface of the test piece which was traversed by the boundary would be roughened, and this was the writer's expectation. But, against this expectation, this part of the surface of the test piece becomes rather smoothed when compared with the other part, as will be seen in the photograph. This point, together with the fact that the grooves are formed only at the initial and final position of the inter-crystalline boundary, seems to be acceptable by considering in the following way: The formation of the groove at high temperature requires some duration of time. At the end of the recrystallization the inter-crystalline boundary does not move no more and it has sufficient time at its fixed position to be grooved, and at the beginning the start of the displacement of the inter-crystalline boundary commences after a lapse of the time and during which the grooving of the inter-crystalline boundary arises. The displacement of inter-crystalline boundary which is obtained with the recrystallization, at such a high temperature as is very near to the melting point, as in the present experiments, takes place very rapidly. Therefore, the inter-crystalline boundary moves very swiftly, without having sufficient time to be grooved, beneath the surface liquid layer which was formed at such a high temperature; and small surface irregularities of the test

piece which have existed initially, become rather smoothed by the displacement of the intersection of the inter-crystalline and the surface liquid layers. The writer carried out similar experiments with aluminium, and the results were entirely the same as with tin.

§ **VII** *Conclusion.* By the present investigation it becomes now clear that with various metals the inter-crystalline boundary and the outer surface of the test piece fluidify at the temperature lower than $10^\circ \sim 20^\circ$ C below the melting point. This phenomenon is seen to take place with metals of very high purity as well as commercial ones, irrespectively whether the test piece is prepared by recrystallizaton or casting. Thus, it is inconceivable to be due to the presence of some impurities, and is rather appropriate to ascribe it to the proper nature of the metal crystals. According to the writer's measurement the inter-crystalline liquid layer becomes pretty thin at the temperature of about $10^\circ \sim 20^\circ$ C below the melting point, differing somewhat with the kind of metals, and below that temperature its presence could not be detected by the method of the present investigation.

With respect to this point it is improbable that the inter-crystalline liquid layer disappears abruptly at a certain definite temperature by cooling. Contrary to this, it seems to be more appropriate to consider after Prof. U. Yoshida that the inter-crystalline layer persists, as in liquid state or as in amorphous solid state, through all temperatures, even when it only becomes thinner with the lowering of the temperature.

As was stated before, the inter-crystalline boundary gets grooved by being heated at high temperature, and it has now become probable from the present investigation that this is due to the sucking of the inter-crystalline liquid layer to the outer surface (probably the interstice between the oxide film and the crystal beneath it) of the test piece by the action of the surface tension. It was found with bismuth that the expansion arising from the crystallization of the inter-crystalline liquid layer by cooling gives rise to the bulging of the neighbouring part of the test piece on one hand and the eruption as small spheres of still uncrystallized part of the liquid layer on the other hand.

Further the writer recrystallized the test pieces of tin and aluminium at such high temperature as to be grooved at the inter-crystalline boundary, and the trace left on the surface of the test piece by the displacement of the inter-crystalline boundary was seen to be comprehensible, at least to some extent, by an explanation based on the presence of liquid layers at the inter-crystalline boundary and on the outer surface of the test piece at high temperature.

Lastly the writer's sincere thanks are due to Prof. U. Yoshida, under whose kind supervision the present investigation was carried out.

Further it must be noted that the expense of this research has been defrayed from the Scientific Research Fund of Department of Education.

(June 20, 1945)

Plate II

Fig. 1 Grooves formed at Al crystalline boundaries.

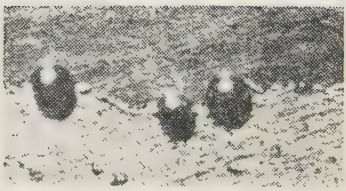

Fig. 2 Crystalline boundary of Bi (sudden cooling)

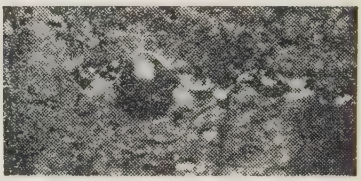

Fig. 3 Crystalline boundary of Bi (slow cooling)

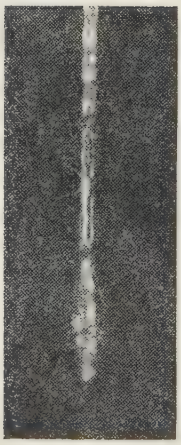

Fig. 4 Bulge formed at lower end of Al plate.

Fig. 5 (a)

Fig. 5 (b)

Displacement of inter-crystalline boundaries.

Memoirs of the College of Science, University of Kyoto, Series A,
Vol. XXV, No. 2, Article 10, 1949.

On the Possibility of Barkhausen-Kurz Oscillation. II

By

Isao Takahashi

(Received November 19, 1946)

1. Introduction

While in the previous paper[1] with the same title the author treated the case when no electrons are caught by the anode in Barkhausen-Kurz tube, in this paper, the interelectrode current of Barkhausen-Kurz tube is calculated in the case when the electrons of larger amplitude are captured by the anode and the occurrence of negative resistance is demonstrated in some numerical examples.

2. Currents between Electrodes, when the Electrons of larger Amplitude are captured by the Anode.

We consider this case for (a) and (b) with the anode d. c. voltage $V_a = 0$ in Fig. 1. The amplitude d_m of an electron from G to A can be obtained by means of u_2 in Part I:

$$\begin{aligned} d_m - d_2 &= \frac{\beta_2}{\omega^2} e^{j\omega(t_0+T_1)}\left(e^{j\omega T_2} - 1 - j\omega T_2\right) \\ &\quad + \frac{T_2}{T_1}\frac{\beta_1}{\omega^2} e^{j\omega t_0}\left(e^{j\omega T_1} - 1 - j\omega T_1 e^{j\omega T_1}\right) \\ &= \frac{\beta_2}{\omega^2}\gamma e^{j(\omega t_0 - \varphi)}, \end{aligned} \tag{1}$$

where $\beta_1 = \dfrac{ev_1}{md_1}$ for (a) and (b), and

$$\beta_2 = \begin{cases} \dfrac{ev_1}{md_2} & \text{for (a)} \\ \dfrac{-ev_2}{md_2} & \text{for (b)} \end{cases}$$

and T_1 is the transit time from K to G, while T_2 is the transit time

1. I. Takahashi: On the possibility of Bankhausen-Kurz oscillation, I. This Memoirs, A, Vol. **25**, No 1, Article 3, 1947.

from G to the turning point. Thus the electrons leaving K at t_0 which makes the real part of (1) positive, that is, which satisfies

$$\left(2N - \frac{1}{2}\right)\pi < \omega t_0 + \varphi < \left(2N + \frac{1}{2}\right)\pi,$$

are destined to be caught by the anode, and the electrons starting at t_0 which makes the real part of (1) negative, that is, which satisfies

$$\left(2N + \frac{1}{2}\right)\pi < \omega t_0 + \varphi < \left(2N + \frac{3}{2}\right)\pi,$$

are to turn back in front of the anode.

Now, we know that the function $f(\omega t_0 + \varphi)$ such that

$$f(\omega t_0 + \varphi) = 0 \quad \text{for} \left(2N - \frac{1}{2}\right)\pi < \omega t_0 + \varphi < \left(2N + \frac{1}{2}\right)\pi,$$

and

$$f(\omega t_0 + \varphi) = 1 \quad \text{for} \left(2N + \frac{1}{2}\right)\pi < \omega t_0 + \varphi < \left(2N + \frac{3}{2}\right)\pi,$$

is expressed as:

$$f(\omega t_0 + \varphi) = \frac{1}{2} + \frac{2}{\pi}\left(-\frac{\cos(\omega t_0 + \varphi)}{1} + \frac{\cos 3(\omega t_0 + \varphi)}{3} \cdots\cdots\right)$$

$$= \frac{1}{2} + F(t_0) \qquad (2)$$

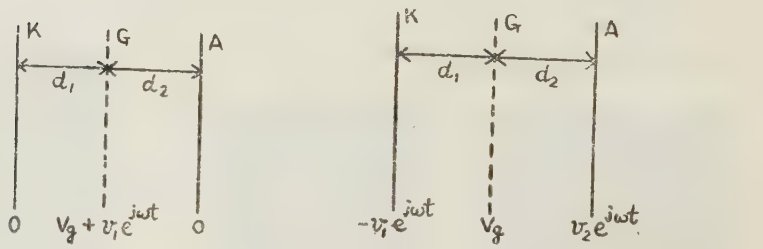

A: anode
G: grid
K: cathode

V_g: positive grid voltage
$ve^{j\omega t}$: oscillating voltage
d: distance between electrodes

Fig. 1. Voltage distribution

We distinguish two classes of electrons. The first class consists of electrons which are not caught by the anode, thus being emitted by K in $n\{1/2 + F(t_0)\}$ per unit time, and the second class consists of electrons which are caught by the anode, thus being emitted in $n\{1/2 - F(t_0)\}$

per unit time. We proceed as in Part I. The current J_A flowing into G from outside on account of electron motions between G and A is

$$J_A = -\frac{ne}{d_2}\int_{t-T_1-\delta T_1'-\delta T_1''-\delta T_2''}^{t-T_1-\delta T_1'}\left(\frac{1}{2}+F(t_0)\right)u_2 dt_0 - \frac{ne}{d_2}\int_{t-T_1-T_2-\delta T_1'-\delta T_4'}^{t-T_1-\delta T_1'}\left(\frac{1}{2}-F(t_0)\right)u_2 dt_0,$$

where δT_4 is included in the instant $t = t_0+T_1+T_2+\delta T_1(t_0)+\delta T_4(t_0)$ at which the second class electron reaches A and $\delta T_4'$ is equal to $\delta T_4(t-T_1-T_2)$. Then, the d.c. part of J_A' is

$$J_1' = -\frac{ne}{d_2}\left\{\int_{t-T_1-T_2}^{t-T_1}\frac{1}{2}u_2' dt_0 + \int_{t-T_1-2T_2}^{t-T_1}\frac{1}{2}u_2' dt_0\right\} = -\frac{nea_2}{4d_2}T_2^2$$

and the a.c. part of frequency ω of J_A' is

$$\begin{aligned} i_1' = -\frac{ne}{d_2}\Bigg\{&\int_{t-T_1-2T_2-\delta T_1''-\delta T_2''}^{t-T_1-2T_2}\frac{1}{2}u_2' dt_0 + \int_{t-T_1-2T_2}^{t-T_1}\frac{1}{2}u_2'' dt_0 - \int_{t-T_1-2T_2}^{t-T_1}\frac{2}{\pi}\cos(\omega t_0+\varphi)\,u_2' dt_0 \\ &-\int_{t-T_1-\delta T_1'}^{t-T_1}\frac{1}{2}u_2' dt_0 + \int_{t-T_1-T_2-\delta T_1'-\delta T_4'}^{t-T_1-T_2}\frac{1}{2}u_2' dt_0 + \int_{t-T_1-T_2}^{t-T_1}\frac{1}{2}u_2' dt_0 \\ &+\int_{t-T_1-T_2}^{t-T_1}\frac{2}{\pi}\cos(\omega t_0+\varphi)\,u_2' dt_0 - \int_{t-T_1-\delta T_1'}^{t-T_1}\frac{1}{2}u_2' dt_0\Bigg\}. \end{aligned}$$

Thus

$$\begin{aligned} i_1' = &-\frac{ne}{d_2\omega^2}\frac{2a_2}{\pi}e^{j\omega t}\left\{e^{j\varphi}\left(e^{j\omega T_1}+1+j\omega T_2 e^{j\omega T_1}\right)\right\} \\ &+\frac{ne}{d_2\omega^2}\beta_1 e^{j\omega t}\Bigg\{\left(\frac{2a_1+a_2}{2a_1}\right)\left(1-e^{j\omega T_1}-j\omega T_1 e^{-j\omega T_1}\right)e^{-j2\omega T_2} \\ &-j\omega T_2\left(1-e^{-j\omega T_1}\right)e^{-j2\omega T_2} \\ &+\left(1-e^{-j\omega T_1}-j\omega T_1 e^{-j\omega T_1}\right) \\ &-\frac{1}{2}\left(2-e^{-j\omega T_1}-e^{-j2\omega T_2}\right) \\ &\times\left[\left(\frac{a_1+a_2}{a_1}\right)\frac{\left(1-e^{-j\omega T_1}-j\omega T_1 e^{-j\omega T_1}\right)}{j\omega T_1}-\left(1-e^{j\omega T_1}\right)\right] \\ &+\frac{1}{2}\frac{\beta_2}{\beta_1}\left(1-e^{-j2\omega T_2}-j2\omega T_2 e^{-j2\omega T_2}\right) \\ &+\frac{1}{2}\frac{\beta_2}{\beta_1}\left(2-e^{-j\omega T_1}-e^{j2\omega T_2}-j3\omega T_2\right)\Bigg\}, \end{aligned} \qquad (3)$$

where $a_1 = \frac{eV_g}{md_1}$, $x_2 = \frac{eV_g}{md_2}$.

The current J_K flowing into G from outside on account of electron motions between K and G is

$$J_K = \frac{ne}{d_1}\int_{t-T_0-\delta T_0'}^{t-T_1-2T_2-\delta T_1''-\delta T_2''}\left(\frac{1}{2}+F(t_0)\right)u_3\,dt_0 .$$

Then, J_2', the d. c. part and i_2', a. c. part of frequency ω are respectively:

$$J_2' = \frac{ne}{d_1}\left\{\int_{t-T_0}^{t-T_1-2T_2}\frac{1}{2}u_3'dt_0 + \int_{t-T_1}^{t}u_1'dt_0\right\} = \frac{nex_1}{4d_1}T_1^2,$$

$$i_2' = \frac{ne}{d_1}\left\{\int_{t-T_0-\delta T_0'}^{t-T_0}\frac{1}{2}u_3'dt_0 + \int_{t-T_0}^{t-T_1-2T_2}\frac{1}{2}u_3''dt_0 - \int_{t-T_0}^{t-T_1-2T_2}\frac{2}{\pi}\cos(\omega t_0+\varphi)\,u_3'dt_0\right.$$

$$\left. - \int_{t-T_1-2T_2-\delta T_1''-\delta T_2''}^{t-T_1-2T_2}\frac{1}{2}u_3'dt_0 + \int_{t-T_1-\delta T_1'}^{t-T_1}u_1'dt_0 + \int_{t-T_1}^{t}u_1''dt_0\right\}.$$

Thus, we have

$$\begin{aligned}
i_2' = {} & -\frac{ne}{d_1\omega^2}\frac{2d_1}{\pi}e^{j\omega t}\left\{e^{j\varphi}(1-e^{j\omega t}+j\omega T_1 e^{j\omega T_1})\right\} \\
& + \frac{ne}{d_1\omega^2}\beta_1 e^{j\omega t}\left\{\left(\frac{2a_1+a_2}{2a_2}\right)(1-e^{-j\omega T_1}-j\omega T_1 e^{-j\omega T_1})\,e^{-j2\omega T_2}\right. \\
& \quad -j\omega T_2(1-e^{-j\omega T_1})\,e^{-j2\omega T_2} \\
& \quad +(1-e^{-j\omega T_1}-j\omega T_1 e^{-j\omega T_1}) \\
& \quad +\frac{1}{2}\left[3(1-e^{-j\omega T_1}-j\omega T_1) \right. \\
& \qquad -(1-e^{-j\omega T_1})^2 e^{-j2\omega T_2} \\
& \quad \left.\left. -\frac{a_1+a_2}{a_2}\frac{2(1-e^{-j\omega T_1})(1-e^{-j\omega T_1}-j\omega T_1)\,e^{-j2\omega T_2}}{j\omega T_1}\right] \right. \\
& \quad +\frac{1}{2}\frac{\beta_2}{\beta_1}(1-e^{-j2\omega T_2}-j2\omega T_2 e^{-j2\omega T_2}) \\
& \quad +\frac{1}{2}\frac{\beta_2}{\beta_1}(1-e^{-j\omega T_1})\times\left[(1-e^{-j2\omega T_2}) \right. \\
& \qquad \left.\left. -\frac{a_1+a_2}{a_2}\frac{(1-e^{-j2\omega T_2}-j2\omega T_2 e^{-j2\omega T_2})}{j\omega T_2}\right]\right\}
\end{aligned}$$

Now, the total d. c. current becomes

$$J_1' + J_2' = \frac{ne}{4}\left(\frac{a_1}{d_1}T_1^2 - \frac{a_2}{d_2}T_2^2\right) = 0\,, \tag{4}$$

because of $a_1T_1 = a_2T_2$.

3. Some Numerical Examples

i_1' and i_2' consist respectively of two components, one of which contains the factor α and the other the factor β.

We attach the suffixes a and b to i_1' and i_2' for the cases (a) and (b) in Fig. 1 respectively. For (b) $-i_{1b}'$ is chosen instead of i_{1b}', on account of the sign of the oscillating voltage between G and A.

Hence

$$i_{1a}' = \frac{ne}{d_2\omega^2}\frac{2a_2}{\pi}e^{j\omega t}(A_1 + jB_1) + \frac{ne}{d_2\omega^2}\beta_1 e^{j\omega t}(R_1 + jI_1),$$

$$i_{2a}' = \frac{ne}{d_1\omega^2}\frac{2a_1}{\pi}e^{j\omega t}(A_2 + jB_2) + \frac{ne}{d_1\omega^2}\beta_1 e^{j\omega t}(R_2 + jI_2),$$

$$-i_{1b}' = \frac{ne}{d_2\omega^2}\frac{2a_2}{\pi}e^{j\omega t}(A_3 + jB_3) + \frac{ne}{d_2\omega^2}\beta_1 e^{j\omega t}(R_3 + jI_3),$$

$$i_{2b}' = \frac{ne}{d_1\omega^2}\frac{2a_1}{\pi}e^{j\omega t}(A_4 + jB_4) + \frac{ne}{d_1\omega^2}\beta_1 e^{j\omega t}(R_4 + jI_4),$$

and we obtain the following table:

ωT_1	ωT_2	A_1	R_1	A_2	R_2	A_3	R_3	A_4	R_4
$\frac{\pi}{2}$	$\frac{\pi}{2}$	+0.57	+0.66	+0.57	+0.52	−0.30	+4.43	−1.11	+2.03
$\frac{\pi}{3}$	$\frac{2\pi}{3}$	−2.22	+3.16	+0.49	−0.32	−1.80	+2.65	−0.43	+0.00
$\frac{\pi}{4}$	$\frac{3\pi}{4}$	−0.97	+9.72	+0.30	−0.13	−2.36	+1.43	−0.12	−0.26

As the first terms in i_1' and i_2' are larger in magnitude than the second terms, corresponding to the ratio of α to β, so we expect the oscillation, when both A's are negative, that is, for $-i_{1b}'$ and i_{2b}' in these examples. Here are presented only the possibility of oscillation but not the limit of oscillation.

Memoirs of the College of Science, University of Kyoto, Series A,
Vol. XXV, No. 2, Article 11, 1949.

A Note on the Angular Distribution of Pair-electrons of 17 Mev γ-Rays.

By

Sakae Shimizu and Jiro Muto.

(Received February 10, 1948)

In conjunction with other members of our laboratory we reported previously[1] the results of the cloud chamber observation of photo-alpha particles expelled from a lead plate under the irradiation of 17 Mev γ-rays of Li (p-γ) reaction. Examining the photographic films taken in that experiment, we obtained 36 comparatively clear tracks of electron-pairs emitted from a lead plate of 1 mm in thickness. We have measured the angular distribution of partners of the pairs with respect to the incident 17 Mev photons. We are giving here a brief note on the results obtained.

According to H. Bethe[2] the angular distribution is given by

$$\Phi(\theta)\,d\theta = \frac{\theta d\theta}{(\Theta^2+\theta^2)^2}\,, \quad \Theta = \frac{mc^2}{mc^2+E}\,, \qquad (1)$$

where θ is the angle between the direction of the emitted electron and that of the incident γ-rays, and E is the kinetic energy of that electron. Since, however, we measured only the angular distribution of the projection of the tracks upon the horizontal plane, the formula was adequately modified so as to be comparable directly with the experimental results.

Thus,

$$\psi(\theta')d\theta' = \frac{d\theta'}{\pi}\int_{\theta'}^{\pi/2}\frac{\Phi(\theta)\,d\theta}{\sqrt{1-(\theta'/\theta)^2}} = \frac{d\theta'}{\pi}\int_{\theta'}^{\pi/2}\frac{d\theta}{(\Theta^2+\theta^2)^2\sqrt{1-(\theta'/\theta)^2}}\,, \qquad (2)$$

and we obtained, as the final theoretical expression,

$$\Psi(\theta')d\theta' = d\theta'\int\psi(\theta',E)\,W(E)dE, \qquad (3)$$

where $W(E)$ is the probability that the kinetic energy of the produced

electron lies between E and $E + dE$. The integration was numerically carried out by using the theoretical value of $W(E)$ given by H. Bethe and W. Heitler.[3]

In Fig. 1 the experimental results are compared with the theoretical values. It is found at once that the number of electrons emitted in angle less than 10° are considerably small in comparison with that of theoretical expectation. This fact may be explained by some reasons such as the effects of the thickness of the lead plate and the difficulties of distinguishing tracks of single electron from those of pair of electrons of very small angle. Since the total number of the tracks is small, we cannot affirm something about the angular distribution of the pair-electrons definitely. We may announce, however, that for very high energy γ-rays as 17 Mev, the agreement between the experiment and the theory seems satisfactory. Further observation is now in preparation.

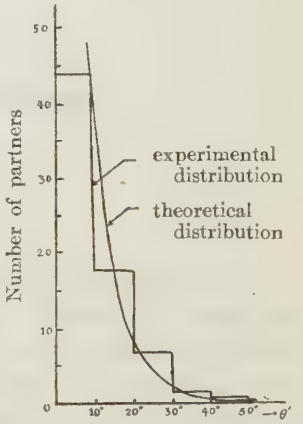

Fig. 1. Distribution of the angle between the partners of the pairs and the photons of 17 Mev γ-rays.

We wish to express our thanks to Professor B. Arakatsu for his encouragement and guidance during this work.

Institute of Physics, University of Kyoto.

November, 1947.

Literatures.

1. B. Arakatsu, S. Shimizu, T. Hanatani and J. Muto, Journ. Phys. Soc., Japan, **1**, 24 (1946).
2. H. Bethe, Proc. Cambridge. Phil. Soc., **30**, 524 (1934).
3. H. Bethe and W. Heitler, Proc. Roy. Soc., London, A, **146**, 83 (1934).

Memoirs of the College of Science, University of Kyoto, Series A,
Vol. XXV, No. 2, Article 12, 1949.

On the Ultraviolet Radiation from the Solar Corona. II.

By

Shotaro Miyamoto and Satoshi Matsushima.

(Received April 10, 1947)

§ 5. *Ionization of He I.* Denote by B_{1c} the absorption coefficient from the ground level 1 of *He I* to the continuous level c. We assume it to be equal to the value at the series limit with the effective range Δ_ν. Then we can write[4]

$$B_{1c} = \frac{4\pi^2 e^2}{mch\nu\Delta_\nu} f \ , \qquad (5,1)$$

in which $f = 1.55$ and $\Delta_\nu = 9.75 \times 10^{15}$.

Let A_{c1} and B_{c1} be the Einstein coefficients for the transition $c \to 1$. Then, we have, by the well-known consideration of thermodynamical equilibrium,

$$\frac{B_{1c}}{B_{c1}} = \frac{4(2\pi mkT)^{3/2}}{h^3} \ , \ A_{c1} = \sigma_\nu B_{c1}\Delta_\nu \ , \ \sigma_\nu = \frac{2h\nu^3}{c^2} \ , \qquad (5,2)$$

where T means the electron temperature of the chromosphere. We shall safely assume it to be equal to the effective temperature of photosphere.

Let N_e, N and N^+ be the particle density of electron, *He I* and *He II* respectively, and J_ν, the mean intensity of the coronal ν-radiation. Then, the equation of ionization is given by

$$N_e N^+ q A_{c1} = N B_{1c} J_\nu \Delta_\nu \ , \qquad (5,3)$$

where we have introduced the factor q in order to include the capture to the excited levels. This becomes, by using (5,2),

$$\frac{N_e N^+}{N} = \frac{4(2\pi mkT)^{3/2}}{qh^3\sigma_\nu} J_\nu . \qquad (5,4)$$

As for J_ν, it changes with the depth, since the chromosphere is not transparent to the coronal radiation. We shall first calculate the optical depth of the chromosphere. The optical depth at the height z is, by definition,

$$\tau = \int_z^\infty \frac{h\nu}{4\pi} B_{1c} N(z)\, dz\,. \qquad (5,5)$$

Following A. Unsöld[5], assume the density distribution of the lower chromosphere to be of the form:

$$N(z) = N(0)\,(0.982e^{-az} + 0.018e^{-a'z})\,, \qquad (5,6)$$

where

$$a = 5.9 \times 10^{-8}\mathrm{cm}^{-1}\ ,\ a' = 2.6 \times 10^{-8}\mathrm{cm}^{-1}\,.$$

We shall first consider $N(z)$ to be the particle density of the total gas, or practically that of hydrogen. It is not known exactly. In the following, we shall treat three cases: $\log N(0) = 16$, 15 and 14. *He* abundance is also not known accurately. Using Payne's estimation[6] from the stellar data, we take for the logarithm of the relative abundance of *He* to *H* to be -2.7. Thus, we shall consider for H_e the following three cases: $\log N(0) = 13.3$, 12.3 and 11.3.

As will be seen later, *He* ionization is weak throughout the chromosphere, so that we can consider (5,6) as the distribution of H_e *I*. The optical depth , (5,5), is then expressed by this and (5,1) as follows:

$$\tau = \frac{\pi e^2 f}{mc\Delta_\nu} N(0)\left(\frac{0.982}{a}e^{-az} + \frac{0.018}{a'}e^{-a'z}\right). \qquad (5,7)$$

With this formula we find for the optical thickness $\tau_1 = 1500$, 150, 15, corresponding to $\log N(0) = 13.3$, 12.3 and 11.3 respectively.

Coronal radiation will be absorbed or scattered in the chromosphere. In place of the exact treatment of the problem, we shall consider two extreme cases: namely, the case of pure absorption and of pure scattering. As is easily seen by the rough estimation, the probability of de-excitation from the excited level of *He I* by the electron collision is larger than that of ionization and capture. Therefore, the actual condition in the chromosphere may be near to the case of pure absorption.

In the case of pure absorption, we have at once

$$J_\nu = J_\nu^* e^{-\tau}\,, \qquad (5,8)$$

while in the case of pure scattering, it can easily be shown that

$$J_\nu = J_\nu^*\,(\,5 - 2e^{-\tau}\,)\,, \qquad (5,9)$$

where we have denoted by J_ν^* the mean intensity of incident coronal light.

§ 6. The ionization formula (5,3) combined with (5,8) becomes

$$\frac{N_e N^+}{N} = 3.1 \times 10^5 e^{-\tau}\,. \qquad (6,1)$$

In the numerical calculation we have taken $q = 2$ and $T_e = 10^6$. Assume that the distribution of the free electron follows the law (5,6), with Cillié and Menzel's estimation[2] $N_e(0) = 4 \times 10^{11}\,\mathrm{cm}^{-3}$ at the base. Then, for $N_e \sim 10^9\,\mathrm{cm}^{-3}$ and $e^{-\tau} \sim 1$ near $z = 1000\,\mathrm{km}$ we have $N^+/N = 3 \times 10^{-4}$.

Population N' of the excited levels are connected with the ionized level by the usual Saha formula:

$$\frac{N_e N^+}{N'} = K(T)\,. \qquad (6,2)$$

Observed *He* spectra are emitted by the scattering of the photospheric radiation. They are thus proportional to N' and hence to NJ_ν, according to (6,2). Three light curves in Fig. 1 represent the quantity

$$E(z) = \frac{N(z)}{N(0)} e^{-\tau}\,, \qquad (6,3)$$

for $\log N(0) = 13.3, 12.3$ and 11.3 respectively. At the great height, $E(z)$ decreases with $N(z)$, while at the deeper layers, it again decreases, since the coronal radiation is weakened rapidly by the absorption. $E(z)$ thus takes a maximum at certain height.

Integrating $E(z)$ to the line of sight, we obtain the quantity directly comparable to the intensity of the flash. The heavy curves in Fig. 1 represent the result of integration. The height of the maximum is shifted scarcely, but there remains a considerable order of intensity even at the base $z = 0$.

A. Pannekoek and M. Minnaert[7] have observed that the *He* inten-

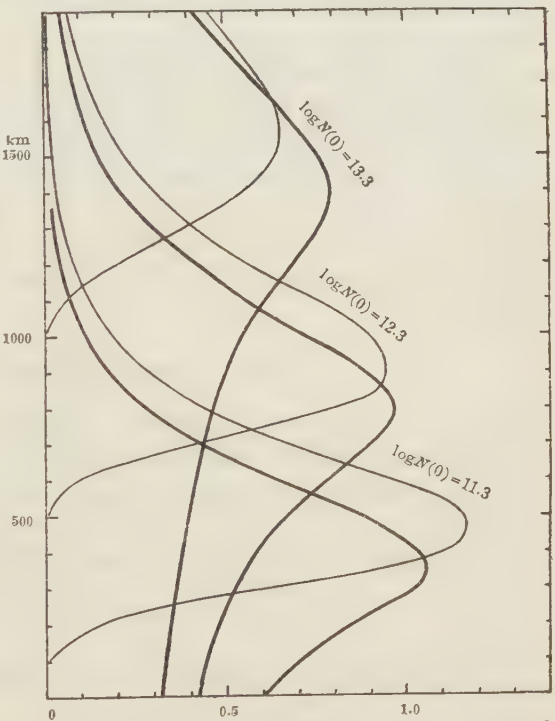

Fig. 1 light curves: $E(z)$, scale unit 2×10^{-4}, 10^{-3} and 10^{-2}
heavy curves: Integrated quantity, scale unit 10 km, 100 km and 1000 km, each for $\log N(o) =$ 13.3, 12.3 and 11.3 respectively.

sity increases with height and first above ~ 1000 km it begins to decrease. Appearance of the maximum is also observed by E. J. Perepelkin and O. A. Melnikov[8] in D_3-line. Theoretically, the maximum place is a function of the chromospheric density. It occurs near 1000 km for $\log N(0) = 12.3$.

So far, we have neglected the absorption due to the neutral hydrogen. It must be taken into account for the lower chromosphere. The absorption decreases rapidly with increasing height, since the hydrogen begins to ionize. Consideration of this effect will not change our conclusion.

In the case of pure scattering, coronal radiation takes a constant intensity throughout the chromosphere. Consequently, there appears no maximum. When the hydrogen absorption is effective, coronal radiation will be weakened in the lower chromosphere and again we can expect a maximum.

§ 7. *Concentration of the excited atom.* We shall make some estimation about the absolute density of the excited *He* atoms, which can be compared with those deduced from the flash observation. At the height ~ 1000 km and for $\log N(0) = 12.3$, we have, as before, $\log N^+/N = -3.5$. Next, by (6,2) with $\chi = 4.74 eV$ for the ionization potential from the excited level, we have $\log N^+/N' = 6.5$. Therefore, $\log N'/N = -10$ and with $\log N = 10$, we have $N' \sim 1\,\mathrm{cm}^{-3}$. These figures are in accord with observation in their order of magnitudes.

§ 8. *Ionization of He II.* Ionization formula for *He II* can be written as

$$N_e N^{++} q^+ A_{c1} = N^+ B_{1c} J_\nu \Delta_\nu \,, \tag{8,1}$$

where J_ν^+ is the mean intensity at the limit of *He II* ionization $\chi = 54.14\, eV$ and other notations are parallel to (5,3).

The probability of absorption per sec per atom is given by

$$B_{1c} J_\nu \Delta_\nu = \int_{\nu_0}^{\infty} B_{1c}(\nu) J_\nu d\nu \,, \quad B_{1c}(\nu) = \frac{2^8 \pi^5}{3\sqrt{3}} \frac{m Z^4 \varepsilon^{10}}{ch^7 \nu^4} \cdot (Z = 2) \tag{8,2}$$

Coronal intensity J_ν is given by (4,1). Introducing it into (8,2), we get

$$B_{1c} J_\nu \Delta_\nu = \frac{2^9 \pi^4 m Z^4 \varepsilon^{10}}{3\sqrt{3}\, ch^7} \frac{C}{T_e^{1/2}} \left(\frac{h}{kT_e}\right)^3 \int_{h\nu_0/KTe}^{\infty} \frac{e^{-x}}{x^4} dx \tag{8,3}$$

For the capture probability, we have

$$A_{ci} = \frac{2^9\pi^5}{(6\pi)^{3/2}} \frac{\epsilon^{10}}{m^2c^3h^3} \left(\frac{m}{k}\right)^{3/2} Z^4 e^{\frac{h\nu}{kT}} \frac{1}{T^{3/2}} E_i\left(\frac{h\nu}{kT}\right). \qquad (8,4)$$

Using these expressions and taking $q^+ = 2$, $T_e = 10^6$, $T = 5600$, we get for (8,1),

$$\frac{N_e N^{++}}{N^+} = 2.1 \times 10^5 . \qquad (8,5)$$

Owing to its small concentration, *He II* is transparent to the coronal radiation near 54.14 *eV*, but it will be weakened in the lower chromosphere by the absorption due to *He I* and *He II*.

λ 4686 of *He II* is emitted by the capture. Its intensity may be proportional to $N_e N^{++}$, which, in turn, is proportional to N^+ by (8,5). According to (6,1), N^+ is proportional to N/N_e at great height. Thus, a slow decrease of λ 4686 with increasing height can be expected, in accord with observation.

In § 4, it has been shown that the contact temperature raises to $T = 16500$ at $\chi = 54.14\,eV$. If we make the formal application of Saha's formula, we must take $\Phi(54.14\,eV) = \chi\,5040/T = 16.5$. This is in agreement with the estimation $\Phi = 15.67$ derived by A. Unsöld from other directions.[9]

Institute of Astrophysics,
University of Kyoto, Japan.
9 April 1947.

References

4. J. P. Vinti, Phys. Rev. **44**, 524 (1933).
5. A. Unsöld, Physik der Sternatmosphäre, (1938) Kap. XVII, **98**.
6. C. H. Payne, Stellar Atmosphere, (1825).
7. A. Pannekoek and M. Minnaert, Verh. Akad. Wetensch. Amsterd. (Sect. 1) **13**, Nr. 5 (1928). Cf. also, A. Unsöld, Physik der Sternatmosphäre (1938) Kap. XVII, **98**.
8. E. J. Perepelkin and O. A. Melnikov, Pulkovo Bull., **14**, Nr. 122 (1935). Cf. also, A. Unsöld, *loc. cit.*
9. A. Unsöld, Physik der Sternatmosphäre, (1938) Kap. XVII, **97**.

Memoirs of the College of Science, University of Kyoto, Series A,
Vol. XXV, No. 2, Article 13, 1949.

Microclimatic Study. I.
A New Type Self-Recorder.*

By

Ken-ichi Takasu

(Received January 23, 1948)

I. Introduction.

It is well known in our domain that F. Albrecht designed various devices to record fine registration or tracing of temperature and wind velocity immediately near the ground surface, and that M. Fransilla started systematic microclimatic observation by using combination of resistance thermometer and hot wire anemometer as the preliminary work of physical microclimatic study. Although Fransilla preferred dot-tracing method which appeared more practicable to optical method, the writer used the latter method, since an attachment of the devices could be simplified for out-door manipulations and continuous recording was made possible with an optical recording apparatus.

II. Description of the Apparatus.

(a) **Recording part.** Features of the new type self-recorder designed by the writer are : (i) several small short period galvanometers with high sensibility even when single thermoelement is employed are arranged in short space ; (ii) the whole system is set in a portable case to be suitable for field observation. The galvanometers of oscillographical arrangement with 3 to 6 pole-pieces for one base magnet work as D'Arsonval type. Volt-sensibility of this galvanometer is of order of 10^{-6}. The constants are shown in Table 1.

The recording drum is driven by clockwork and has velocity of 3.6 mm/min (type A) or 6.0 mm/min (type B), and time required for a complete cycle is 1.5 and 1 hr respectively. Distance between galvanometer and drum is 24 cm and 28 cm and changes of six elements are recorded each separately and simultaneously on a bromide paper of 15 cm width up to 0.1° C in temperature. Type A, lighter in weight, requires black cover when the bromide paper needs changed, type B with magazine suitable for operation in open-air adds considerable weight.

* The writer wishes to show his appreciation for the kindness of Prof. Sassa who permitted him to modify the galvanometer for geophysical prospecting, and also for the help given by Mr. I. Yasuda when the apparatus was constructed.

Table 1.

	coil resist.	critical damping resist.	period	volt-sensibility
type A	26 Ω	35 Ω	0.3 sec*	5×10^{-6}
type B	20 Ω	30 Ω	0.6 sec	3×10^{-6}

(b) Measuring part. Thermojunction, hot-wire anemometer and Gorczinsky's solarimeter were connected to galvanometers of the recorder to record temperature, wind-velocity and solar radiation.

(i) Thermojunction: The most difficult point in air temperature measurement is how to remove radiation effect. Especially in case of microclimatic study the problem becomes serious, as employment of radiation screen disturbs natural state of "Austausch". Studies on radiation effect upon thermojunction or resistance thermometer have been reported by some writers, for instance Rossi[1] reported that with a thermoelement of 0.25 mm diameter there exist 0.28° C, 0.48° C and 0.87° C radiation errors under the radiation of 1.5 g cal/cm² min and wind velocity of 3.1 m/sec, 1.1 m/sec and 0.3 m/sec respectively. The writer used exposed thermoelements of diameter 0.20 mm. (B. S. No. 32) the result should be 0.26° C, 0.45° C and 0.83° C higher than actual under the direct ray of 1.5 g cal/cm² min and wind velocity of 3.0 m/sec, 1.0 m/sec and 0.3 m/sec respectively. If, however, direct ray can be avoided, the radiation becomes less than 1/10 and so the error. Actually, screening of direct ray should no change in galvanometer reading, and the junction was exposed without screen under natural environment. The results can be calibrated by the recorded value of solar radiation and wind velocity if required.

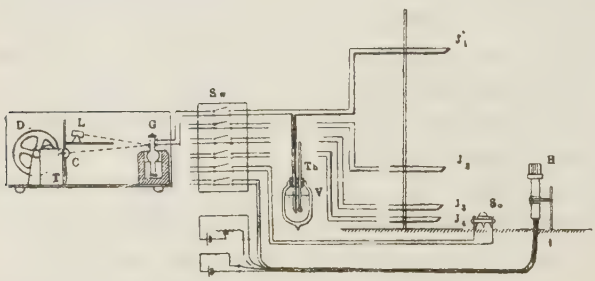

Fig. 1 Schema of the apparatus

Recorder:
G : Galvanometer
L : Light source
D : Revolving drum
T : Clockwork
C : Cylindrical lense

Measuring Part:
J : Thermojunction
H : Hot-wire anemometer
So : Gorczinsky's solarimeter
Th : Thermometer
V : Vacuum flask
Sw : Switch

One of the bundled lead wires of

1. V. Rossi, Mitt. d. Met. Inst. d. Univ. Helsingfors. No. 24 (1933).

junction is extended more than 5 cm. The effect of thermal conduction arisen from temperature difference between lead wire and junction is in most cases not serious as the temperature difference is not so great. It is pointed out here that no foreign metals should come in contact between lead wire and connecting point, and the lead wires are twisted together in bundle to match their resistance to critical damping resistance of the galvanometer.

At ordinary temperature E. M. F. of copper-constantan is proportional to temperature difference, scaling is done simply by inserting the junctions in thermos of known temperature before and after observation and recording the standard line. The cold junction is in water in a thermos, the constant temperature can be maintained as one observation takes only an hour.

(ii) Hot-wire anemometer: The hot-wire anemometer used by the writer is the improved type after Albrecht (1933), and it gives a calibration curve shown in Fig. 2 when standardized against constant known Biram's anemometer in a low-velocity small wind channel. Wind velocity scale on the record was made firstly by taking, before and after the observation, the line of wind velocity ∞, that is, when the heating electric current was cut off, secondly taking that of wind velocity 0, that is, the current and the cap on, and then divided the space between the lines according to the calibration curve. The whole scale must be either magnified or reduced as the case may be.

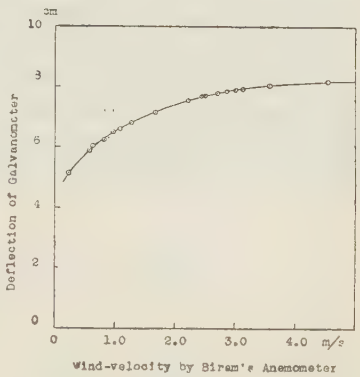

Fig. 2. Calibration curve for the hot-wire anemometer

(iii) Gorczinsky's solarimeter: Calibration of the solarimeter was done by comparison with Kipp & Zonen solarimeter of direct reading type with known constants. Although sufficient accuracy in absolute determination of solar radiation and wind velocity may not be attained, it is satisfactory for the present purpose of the writer, since in most cases only relative change comes into question.

III. Treatment of Records for Microclimatic Study

(i) Following observations were taken by a combination of two recorders as standard, measurment of temperature of the earth surface and of air temperature at 1, 5, 10, 50 and 150 cm above the ground by thermojunction, of wind velocity at 50 and 150 cm. by hot-wire anemo-

meter, and lastly of radiation at the ground surface by Gorczinsky's solarimeter. Choice of the above-mentioned standard elements was sometimes altered and only a part of the observations was done when the case allowed.

(ii) Since recording is simultaneous and continuous, relative change in each elements are shown distinctly and unquestionably. (cf. Fig. 2 a, b, c in Plate 1.)

(iii) Reading of the records should give mean vertical distribution of temperature and index upon proper unit for determination of fluctuation. It is most convenient for this purpose to select the time interval of about 10 min when only the similar changes appear repeatedly. (This selection is also suitable for the purpose of comparing with reading of Assmann's aspiration psychrometer.) If the changes are quite rapid, shorter time interval should be taken. Maximum and minimum values during 15 or 20 sec interval taken as unit upon consideration of time-scale, are read on the record and mean value and range are calculated. Mean vertical distribution is found from the averaged mean value which is the mean value averaged over ten minutes, and index of fluctuation is given by mean value of ranges. An example is shown in Fig. 3, Plate 1 and Table 2.

(iv) Fine registration of temperature and wind velocity can be regarded as record of "Austausch". The method of calculation of "Austausch coefficient" will be discussed in the next section.

(to be continued)

Table 2

Record for 150 cm air temperature (cf. Fig. 3 in Plate 1)

(a)

	Max.	Min.	Mean	Range
Reading of every 15 sec for 12 h 40–41 m	7.6	6.8	7.2	0.8
	9.0	7.8	8.4	1.2
	8.6	7.1	7.9	1.5
	9.4	7.3	8.4	2.1
1 min mean	8.7	7.3	8.0	1.4

(b)

1 min mean	Max.	Min.	Mean	Range
40–41 m	8.7	7.3	8.0	1.4
–42	8.9	7.6	8.3	1.3
–43	10.8	8.6	9.7	2.2
–44	9.5	7.8	8.7	1.7
–45	10.3	8.1	9.2	2.2
5 min mean	9.6	7.9	8.8	1.7

(c)

5 min mean	Max.	Min.	Mean	Range
40–45 m	9.6	7.9	8.8	1.7
45–50	8.5	7.4	8.0	1.1
10 min mean	9.1	7.7	8.4	1.4

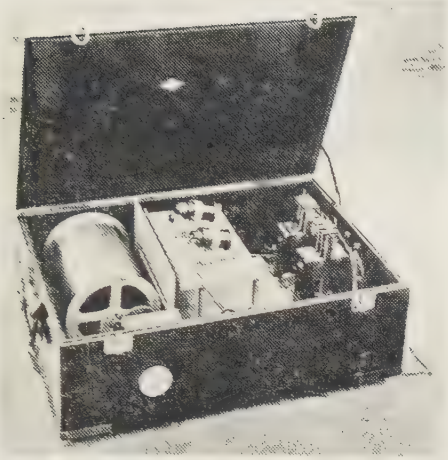

Fig. 1 (a) Recorder Type A

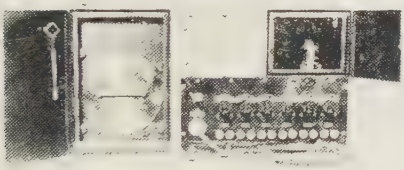

Fig. 1 (b) Recorder Type B

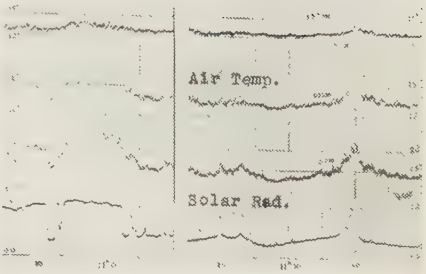

Fig. 2 (a) Temperature change due to the sudden variation of solar radiation (On the grass at the Met Res. Inst., Kyoto Univ. Dec. 7, 1941)

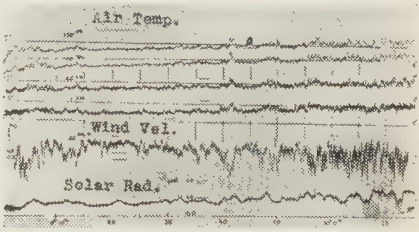

Fig. 2 (b)

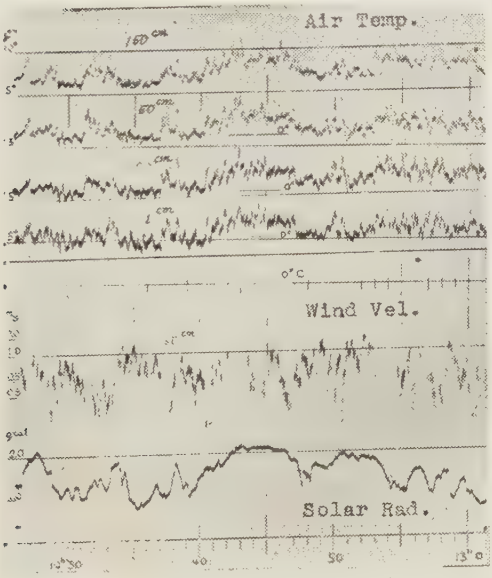

Fig. 3 An example of the record (The same as Fig. 2 b, c)

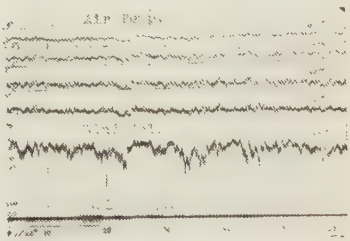

Fig. 2 (c) Temperature rise in daytime (b) and fall at night (c) due to drop of wind velocity
(On the snow-surface at Mt. Shirouma — 1800 m above the sealevel — April 29, 1942)

Memoirs of the College of Science, University of Kyoto, Series A,
Vol. XXV, No. 2, Article 14, 1949.

The Exchange Efficiencies of the Translational and the Internal Energy of Gas Molecules on Solid Surfaces I. Measurement by Means of Molecular Beams

By

Nobuji Sasaki, Kazuhiko Taku and Kazuo Mitani

(Received February 20, 1948)

The energy necessary for the thermal reaction must be carried away from the vessel wall by the cold molecules admitted therein, but, in general, they do not come into thermal equilibrium with the wall by a single collision.[1] The attainment of the state of complete thermal equilibrium might finally be brought about by a mere succession of collisions with the wall. But it may be assisted by the intervention of the mutual collision between gas molecules, for it can average *a priori* very plausible differences in α's for various degrees of freedom of the molecule. Such a view may greatly be supported from the chemical side by a fact previously observed in our laboratory. Namely, the nitrogen pentoxide molecules reserved at 0° C could pass almost undecomposed through a 1 m long glass tube of 3 mm diameter at 100° C and at about 10^{-5} mm Hg, although a simple calculation shows that the molecules could have attained 94° C even with an assumption of impossibly poor exchange efficiency ($\alpha = 0.001$), for it will make as many as about 3000 collisions with the wall during its about 1 sec stay inside the tube. This striking stability may be explained by the extreme difficulty of energy transfer from the wall to the degrees of freedom responsible for the decomposition of the molecule if left alone without mutual collisions. On the other hand, there is every reason to assume that the exchange of the translational energy is almost complete and consequently the actual value of α, though not yet measured, must

1. The efficiency of this energy exchange may be measured by Knudsen's accommodation coefficient α defined by

$$\alpha = \frac{T_2 - T_0}{T_1 - T_0},$$

where T_0 and T_2 are the temperatures of the gas molecules before and after the collision with the wall kept at a temperature T_1. The actual value of α lies rarely below 0.1 and generally increases with the increase of the atomic or the molecular weight.

be much larger than that assumed above, even if all other degrees of freedom had zero exchange efficiency. The knowledge of a for different degrees of freedom is in the chemical kinetics interesting as well as important. Attempts to measure separately the accommodation coefficients for the translational (a_t) and the internal energy (a_i) are not lacking but they are either incomplete or too special.[2] Our method would find general application.

A torsion balance with a mirror M in a vacuum, has a vertically stretched thin metallic ribbon R at T_0 as its one wing, against whose surface gas molecules at T_0 almost perpendicularly collide in a form of horizontal molecular beams to deflect the balance by an angle θ_1. Now the ribbon alone is heated to T_1. The deflection increases from θ_1 to θ_2. If n is the number of gas molecules which impinge on the ribbon per unit time, m the mass of a gas molecule and $\bar{c}_0$ the mean velocity of the gas molecules at T_0, the momentum given to the ribbon per unit time is $am\bar{c}_0n$, where a is the correction factor for oblique collisions made by the molecules in the diverging beams. The momentum given to the ribbon per unit time by the n rebounding molecules is $bm\bar{c}_0n$ when the ribbon is at T_0 and $bm\bar{c}_2n$ when at T_1, where b is the correction factor for the molecules being reflected according to the cosine law, and $\bar{c}_2$ the mean velocity of the molecules leaving the surface maintained at T_1. Hence the total momentum given to the ribbon per unit time is

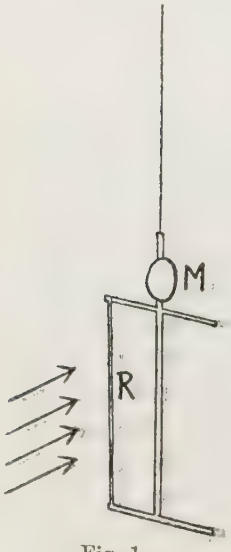

Fig. 1.

$$M_1 = am\bar{c}_0n + bm\bar{c}_0n,$$

when the temperatures of the gas and the ribbon are T_0, and

$$M_2 = am\bar{c}_0n + bm\bar{c}_2n,$$

when the temperature of the gas is T_0 and that of the ribbon T_1.

As M_1/M_2 is equal to θ_1/θ_2, we have

$$\bar{c}_2 = \left\{\left(\frac{a}{b} + 1\right)\frac{\theta_2}{\theta_1} - \frac{a}{b}\right\}\bar{c}_0. \quad \cdots\cdots(1)$$

2. M. Knudsen: Ann. Phys., **6** (1930), 129.
W. R. v. Wijk: Z. Phys., **75** (1932), 584.
L. S. Ornstein and W. R. v. Wyk: Z. Phys., **78** (1932), 734.
H. H. Rowley and K. F. Bonhoeffer: Z. phys. Chem., B **21** (1933), 84.

If the Maxwell's law for the distribution of velocities holds for the departing molecules,

$$(\overline{c_2}/\overline{c_0})^2 = \overline{c_2^2}/\overline{c_0^2} ,$$

where $\overline{c_0^2}$ and $\overline{c_2^2}$ are the mean square velocities of the molecules before and after the collision. Hence we get

$$a_t = \frac{\overline{c_2^2} - \overline{c_0^2}}{\overline{c_1^2} - \overline{c_0^2}} = \frac{\{(a/b + 1)\theta_2/\theta_1 - a/b\}^2 \overline{c_0^2} - \overline{c_0^2}}{\overline{c_1^2} - \overline{c_0^2}} ,$$

or substituting $\overline{c_0^2} = 3RT_0/M$ and $\overline{c_1^2} = 3RT_1/M$, finally,

$$a_t = \frac{[\{(a/b + 1)\theta_2/\theta_1 - a/b\}^2 - 1]T_0}{T_1 - T_0} \quad \cdots\cdots\cdots\cdots(2)$$

The correction factors a and b can be calculated from the geometry of the ribbon and the defining slits for the beams.

To obtain a_i significant for comparison, we at once measure the total loss of heat E cal per sec from one and the same ribbon heated *in situ* in the gas at p mm Hg. The kinetic theory of gases enables us to calculate a_i from E and a_t by

$$a_i = \frac{17.141 \frac{\sqrt{T_0 M}}{pA} E - 3.9738\, a_t (T_1 - T_0)}{(H_1 - H_0) - 2.9804 (T_1 - T_0)} \quad \cdots\cdots\cdots\cdots(3)$$

where A : the surface area of the ribbon in cm^2, compensated for the end effect,

M : the molecular weight of the gas,

H_0, H_1 : the heat contents of the gas at T_0 and T_1 respectively.

To ensure the frictionless deflection in the actual measurement, the ribbon was heated as a part of a closed circuit with a high frequency resonance coil L_1 and a condensor C in series, all built up in the torsion balance, the heating current being induced from outside. The temperature or the resistance of the ribbon was measured by connecting the two free ends of the ribbon-compensator (by raising the levels in the mercury contacts H in the vacuum) and its middle junction point M (via the suspension wire), with the outside circuit through three choke coils L_2, L_3 and L_4 to form a very weak direct current Wheatstone bridge (Fig. 2).

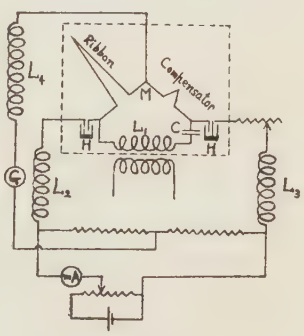

Fig. 2

The results obtained with nitrogen at 31.3° C and a nickel ribbon at 518.0° C are

$$a_t = 0.393 \quad \text{and} \quad a_i = 0.314 \ ,$$

indicating a more efficient exchange for the translational energy in conformity with the results already obtained by other investigators.

The present research was carried out by the grant from the Education Ministry for natural science and the Society of Promotion of Arts and Sciences of Japan. We wish to express our thanks to Mr. S. Mimashi, Dr. E. Nishibori and Dr. O. Mabuchi for their kindly providing us with laboratory facilities.

Laboratory of Inorganic Chemistry,
Institute of Chemistry,
College of Science, Kyoto University.

Memoirs of the College of Science, University of Kyoto, Series A,
Vol. XXV, No. 2, Article 15, 1949.

The Exchange Efficiencies of the Translational and the Internal Energy of Gas Molecules on Solid Surfaces II. Measurement by Means of a Vibrating Hot Filament

By

Nobuji Sasaki and Kazuo Mitani

(Received February 20, 1948)

In the preceding paper a molecular beam method for measuring separately the exchange efficiencies of the translational (a_t) and the internal energy (a_i) of gas molecules was described.[1] The present report is concerned with another new method. Here we make use of a filament F in a A shape, fixed at both ends and capable of heating by an electric current in a glass tube A which can be evacuated to a high vacuum by a mercury diffusion pump. Trap T is cooled with liquid air. The pressure in A is measured by a Mcleod gauge. After baking out the apparatus, hydrogen in R is admitted into A through a capillary gas pipette P to a pressure about 10^{-2} mm Hg. The filament set in vibration by a light knock at the tube, is gradually damped by the internal friction of the filament and the friction with the surrounding gas. The period of half decrement τ is affected by the velocities of the on-coming as well as the departing molecules, irrespective of their internal energy. With the filament at a higher temperature than the gas, the larger value of a_t is directly related with the larger velocity of the departing molecules, so that a_i is a function of τ, which can be found as follows. The motion of the

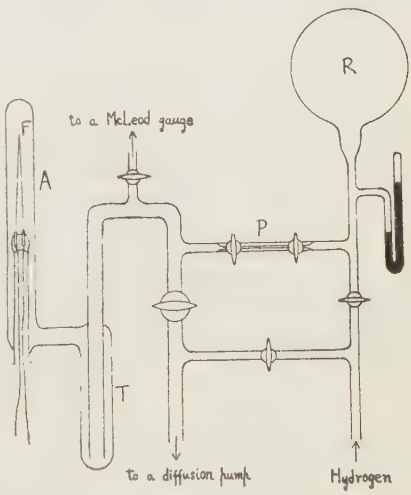

Fig. 1

1. N. Sasaki, K. Taku and K. Mitani: This Memoirs, A, **25** (1949), 70.

heated filament in a gas at a very low pressure may be given by the equation:

$$m_f \frac{d^2x}{dt^2} + r\frac{dx}{dt} + Kx = 0 \ , \quad \cdots\cdots\cdots\cdots (1)$$

where m: the mass of the filament per unit length,
r, k: constants.
From (1) follows

$$r = \frac{2\ln 2}{\tau} m_f \ . \quad \cdots\cdots\cdots\cdots (2)$$

r can be regarded as a sum of r_1 and r_2. While r_1 related to the internal friction of the material of the filament can be determined experimentally, r_2 related to the friction with the surrounding gas can be calculated by the kinetic theory of gases. Thus with a filament of a circular cross-section, the following equation is obtained as a result of a rather lengthy calculation:

$$k_2 \frac{p\sqrt{M}}{T}\sqrt{T + a_t(T_1 - T)}\left\{1 + \frac{(1 - a_t)T}{T + a_t(T_1 - T)} \cdot \frac{1}{3\pi}\right\}$$
$$= \frac{k_1}{\tau} - 1 - \frac{128}{3\pi^3} k_2 \frac{p\sqrt{M}}{\sqrt{T}} \ , \quad \cdots\cdots\cdots\cdots (3)$$

where T, T_1 : the absolute temperatures of the gas and the filament respectively,
p : the pressure of the gas,
M : the molecular weight of the gas,
k_1, k_2 : the constants characteristic of the apparatus to be determined experimentally by various methods.

If the temperature of the filament is equal to that of the gas, the above equation is reduced to the ordinary equation for a quartz fibre manometer deduced by A. Einstein[1]:

$$b = (p\sqrt{M} + a)\tau \ ,$$

where a and b are constants.

Equation (3) transformed into the following form:

$$a_t = \frac{T}{T_1 - \left(1 + \frac{2}{3\pi}\right)T}\left[\frac{T}{k_2^2 p^2 M}\left(\frac{k_1}{\tau} - 1 - 1.376 k_2 \frac{p\sqrt{M}}{\sqrt{T}}\right)^2 - \left(1 + \frac{2}{3\pi}\right)\left\{1 + \frac{(1 - a_t)^2 T}{T + a_t(T_1 - T)} \frac{1}{3\pi(3\pi + 2)}\right\}\right]$$

1. F. Haber and F. Kerschbaum: Z. Elektrochem., **20** (1914), 296.

can be used to calculate a_t by the method of successive approximation, since the last term in the brace is a small correction term.

As for the accommodation coefficient a_i for the internal energy, we measure the total heat loss from the filament heated *in situ* and calculate a_i by equation (3) in the preceding paper.[1]

The result obtained is $a_t = 0.48$ and $a_i = 0.10$, for a tungsten filament at 300° C and hydrogen at 23° C. In this case a_t surpasses a_i to a greater extent than in the preceding paper.

Details of the calculation and the apparatus will appear elsewhere before long.

The present investigation was carried out by the Education Ministry grant for natural science.

Laboratory of Inorganic Chemistry,
Institute of Chemistry,
College of Science, Kyoto University.

---

1. *loc. cit.*

Memoirs of the College of Science, University of Kyoto, Series A,
Vol. XXV, No. 2, Article 16, 1949.

On the Direct Measurement of the Effective Collision Radii of Potassium with Chlorine and Other Gases.

By

Nobuji Sasaki and Kumasaburo Kodera

(Received February 20, 1948)

In the chemical kinetics the problem of the effective collision radii between the chemically reactive molecules is of special interest. By means of their "highly diluted flame" Polanyi and his collaborators[1] claimed to have shown chlorine and sodium to react at a distance greater than the classical collision radius.

By more direct method of molecular beam, we have examined if there be any influence of chemical reactivity on the effective collision radii. The scattering of an atomic beam of potassium was measured in reactive molecules (Cl_2) and in non-reactive molecules (H_2, N_2, O_2 and A) for the sake of comparison. The atomic beam had the cross section 0.01 mm × 1 mm. Its intensity was measured by the Langmuir-Taylor method of surface ionization using a tungsten filament of diameter 0.022 mm. The thinest beam and the finest filament were used to minimize the scattered atoms striking the filament. The intensities of the beam in vacuum I_{o1} and in a gas I_{p1} at a distance l_1 (1.4cm) from the collimating slit and the corresponding values I_{o2} and I_{p2} at a distance l_2 (4.3 cm) from the slit give the mean free path λ of potassium atom by

$$\lambda = \frac{l_2 - l_1}{\ln\left(\frac{I_{o2} I_{p1}}{I_{o1} I_{p2}}\right)},$$

from which the effective collision radius σ may be calculated by the Tait's expression[2] for the mean free path. The results are shown in

1. M. Polanyi and his collaborators: Z. physik. Chem., **B 1**, 3, (1928) et seq., "Atomic Reactions," London (1932) If we use, instead of their seemingly too small value, that estimated by Mais' method for the radius of sodium atom, the said difference disappears. Cf. Table 2, last column.

2. J. H. Jeans, "Dynamical Theory of Gases", 2nd Ed., p. 271 (1916).

Table 1, where T_G represents the temperatures of the scattering gases and σ_K the sums of r_B and r_G in Table 2.

Table 1.

No.	H_2	N_2	O_2	A	Cl_2	T_G
1	7.79Å		12.1Å	12.0Å		112°K
2				11.8Å		112°K
3*	(7.57Å)	(11.5Å)	(11.6Å)			112°K
4	7.32Å	12.2Å	12.0Å	12.3Å		210°K
5					13.5Å	112°K
6					13.4Å	112°K
σ_K	5.0Å	5.5Å	5.4Å	5.4Å	6.1Å	

* The results obtained with a filament of a larger diameter 0.036 mm.

In Table 2, the mean values from Table 1 together with those previously obtained in our laboratory by a different method (No. 1) and by the same method with a beam and a measuring filament of larger dimensions (No. 2 and 3) are given, where r_B means the radii of the beam atoms estimated by Mais[3], r_G the kinetic radii of the scattering gas molecules.

Table 2.

No.	Atomic beam.	Scattering gas.	Observed value σ	Classical kinetic value γ_B	γ_G	σ_K	Ratio σ/σ_K	Other σ
1[4]	Na	Cl_2	5.01	3.0	2.5	5.5	0.91	5.5(Magee) 5.25 (Polanyi)
2[5]	Na	N_2	6.48	3.0	1.9	4.9	1.3	
3[5]	Na	O_2	6.13	3.0	1.8	4.8	1.3	
4[6]	K	N_2	12.2	3.6	1.9	5.5	2.2	
5[6]	K	O_2	12.1	3.6	1.8	5.4	2.2	
6[6]	K	A	12.0	3.6	1.8	5.4	2.2	
7[6]	K	Cl_2	13.5	3.6	2.5	6.1	2.2	8.0(Magee)

Values of σ and γ are in Å unit.

3. W. H. Mais: Phys. Rev., **45**, 773, (1934). The value for sodium was not given by Mais. We estimated it by his own method.

4. N. Sasaki, E. Nishibori and H. Uchida: Journ. Chem. Soc. Japan, **57**, 1277, (1936).

5. N. Sasaki, E. Nishibori, G. Kondo and K. Kodera: ibid., **57**, 1284, (1936).

6. The present report. Also cf. K. Kodera: ibid., **65**, 645, (1944); **66**, 52, (1945); **67**, 80, (1946).

7. J. L. Magee: J. Chem. Phys., **8**, 687, (1940).

Magee[7] estimated the collision (end-on) radii of sodium and the halogen molecules. His theoretical values together with the Polanyi's σ are given in the last column. The collision radius between sodium atom and chlorine molecule (σ_s) was determined by measuring the intensities[8] of the resonance radiation at two spots (9.5 mm apart) along a sodium atomic beam of 2 mm diameter.

In order to consider the meanings of the various kinds of collision radii now at our disposal, a brief account of a result of the quantum mechanical theory of atomic collisions[9] must be introduced. In the case of a rigid body scattering of an atomic beam in a gas, the probability, or more precisely, the "differential" cross section, for the scattering into unit solid angle decreases rapidly, as the angle of scattering increases from zero, from a large value to attain the relatively very small classical cross section at a certain critical angle of scattering (1.4° for potassium and chlorine, and 1.9° for sodium and chlorine) and retains that value for larger angles. Due to this predominance of the small angle scattering the "total" cross section taken all over the scattering angle surpasses the classical value by a factor of 2 to 4.

Putting the angle of demarcation between the large and the small angle scattering at this critical angle, let us compare the various collision radii mentioned above. Beam atoms scattered in large angles (S) may be divided into three parts: (1) those chemically reacted (S_c), (2) those straggled before arriving at the second point of measurement (S_s) and (3) those arriving at the second point (S_a). Beam atoms scattered in small angles may also be divided into three corresponding parts (R_c, R_s and R_a). The letters in parentheses denote qualitatively the portions of the collision radius (σ), which the respective divisions of the scattered atoms may contribute as the manner of measurement varies, so that we have a general formal expression:

$$\sigma = S + R = S_c + S_s + S_a + R_c + R_s + R_a.$$

The classical collision radius σ_k can be given by

$$\sigma_k = S = S_c + S_s + S_a,$$

8. To be correct, these must be multiplied by the atomic velocities to give the beam intensities I's. This correction will reduce the value of σ_s, for the faster atoms are less liable to scattering. On the other hand the pressure of chlorine near the beam must be smaller than the value indicated by the manometer, because the gas is consumed rather vigorously by sodium abundantly depositing on the slits. This correction will increase the value of σ_s.

9. H. S. W. Massey and C. B. O. Mohr, Proc. Roy. Soc., A **141**, 434, (1932).

neglecting its very small classical portion in R; the Polanyi's collision radius σ_p by

$$\sigma_p = S_c + R_c,$$

and our σ_s by

$$\sigma_s = S_c + S_s + R_c.$$

By the way it is to be noted here that, since the cross section of the beam and the second spot of measurement are large, R_s part of the scattered atoms comes to be included in R_a and ceases to contribute to σ. If measured with a very fine beam and a very fine filament as in the case of potassium and chlorine, the radius thus obtained (σ_f) will coincide with the general expression above mentioned:

$$\sigma_f = S_a + R,$$

S_a and R_a parts being nearly zero.

In the case of potassium the ratios σ_f/σ_k in Table 2 are the same for all gases investigated, irrespective of their chemical reactivity and this will certainly be the case with sodium also. This fact excludes the possibility that σ in any way be increased by the existence of chemical reactivity between the colliding particles. The large value 2.2 of σ_f/σ_k may be explained quantum mechanically if some interaction such as van der Waals force exists between the colliding particles. The small value 1.3 is due to the larger measuring tungsten filament which receives larger number of atoms scattered in small angles.

In the case of sodium, if we may assume $\sigma_p = \sigma_s$, then $S_s = 0$, from which necessarily follows $S_a = 0$, so that $\sigma_k = S_c$, finally, if we may put $\sigma_k = \sigma_s$, then $R_c = 0$. The conclusion is approximately: The large angle ($>1.9^\circ$) classical kinetic scattering is all effective in bringing about the chemical reaction between sodium atom and chlorine molecule, while the small angle scattering, or largely quantal scattering, though dominant, is all ineffective.

The present research was carried out by the grant from Education Ministry for natural sciences and the Society of Promotion of Arts and Sciences of Japan (Nippon Gakujutsu Shinko Kai.)

Laboratory of Inorganic Chemistry,
Institute of Chemistry,
Department of Science, Kyoto University.

昭和二十四年十月十五日　印刷
昭和二十四年十月三十日　發行

編輯兼發行者　京都大學理學部

印刷者　河北印刷株式會社
代表者　河北喜四良
京都・二條・堺町

CONTENTS

On a Property of the Conjugate Net in connexion with Generalized Projective Deformation.

BY *Joyo Kanitani* 41

On the Structure of Inter-Crystalline Boundaries of Metals. II

BY *Masaharu Kabata* 45

On the Possibility of Barkhausen-Kurz Oscillations. II

BY *Isao Takahashi* 55

A Note on the Angular Distribution of Pair-electrons of 17 Mev γ-Rays.

BY *Sakae Shimizu* AND *Jiro Muto* 61

On the Ultraviolet Radiation from the Solar Corona. II

BY *Shotaro Miyamoto* AND *Satoshi Matsushima* 63

Microclimatic Study I. A New Type Self-Recorder.

BY *Ken-ichi Takasu* 69

The Exchange Efficiencies of the Translational and the Internal Energy of Gas Molecules on Solid Surfaces I. Measurement by Means of Molecular Beams.

BY *Nobuji Sasaki, Kazuhiko Taku* AND *Kazuo Mitani* 75

The Exchange Efficiencies of the Translational and the Internal Energy of Gas Molecules on Solid Surfaces II. Measurement by Means of a Hot Filament.

BY *Nobuji Sasaki* AND *Kazuo Mitani* 79

On the Direct Measurement of the Effective Collision Radii of Potassium with Chlorine and Other Gases.

BY *Nobuji Sasaki* AND *Kumasaburo Kodera* 83